Nanonis GmbH
www.nanonis.com
info@nanonis.com

Piezoelectric Quartz Tuning Forks for Scanning Probe Microscopy

In this paper the application of piezoelectric quartz tuning forks in dynamic force microscopy is described. For the introduction we give a historical overview and a comparison with traditional cantilevers. In the second section the theories for tuning forks as oscillators for the dynamic force detection are introduced and in the third section the experimental implementation is described. This paper is based on chapter 4 of the dissertation of J. Rychen [1]: "Combined Low-Temperature Scanning Probe Microscopy and Magneto-Transport Experiments for the Local Investigation of Mesoscopic Systems". Swiss Federal Institute of Technology, Diss. ETH No. 14119.

1 Introduction

The tuning fork is one of the best mechanical oscillator. It was invented in 1711 by the english trumpeter John Share. The important mode of the tuning fork is the one where the two prongs oscillate in a mirrored fashion. This has the unique advantage that the center of mass stays at rest and all forces are compensated inside the material connecting the two prongs. Since quartz is one of the materials with the lowest internal mechanical losses, quartz tuning forks have very high quality factors. Furthermore the piezoelectric effect of quartz allows to excite and detect the oscillation of the tuning fork fully electrically. Quartz resonators are widely used as frequency standards and tuning forks are just special examples with high quality factors and low resonance frequency. They are used for example in wrist watches where the insensitivity to accelerations is an additional advantage. Other applications are gyroscopes, micro balances, gas sensors and scanning probe microscopy. Due to the large industrial production they are available at very low cost.

Piezoelectric quartz tuning forks were introduced into scanning probe microscopy by Günther, Fischer and Dransfeld [2] for use in scanning near field acoustic microscopy and later by Karrai and Grober [3] and others [4, 5, 6], as a distance control for a scanning near filed optical microscope (SNOM). In this microscopes the optical fiber tip is oscillating

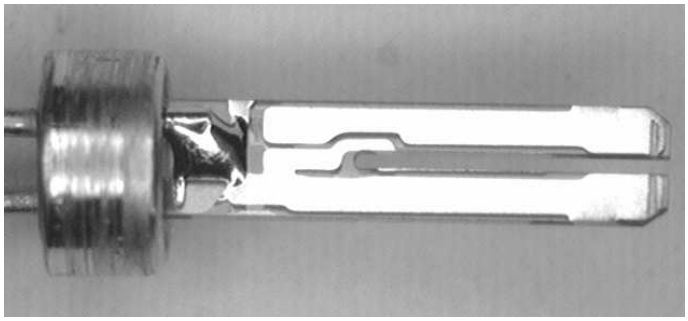

Figure 1: Piezoelectric quartz tuning forks are industrially produced in large numbers and serve as a frequency standard for example in wrist watches. They are packed in a evacuated steel casing and show quality factors of typical 30'000. The type shown is 4mm long and oscillates at 2^{15}Hz = 32768Hz.

parallel to the surface resulting in a shear force detection. Shear forces where then explicitly investigated using tuning forks by Karrai and Tiemann [7]. Quartz tuning forks with a magnetic tip were also used for magnetic force microscopy [8, 9]. Rensen et al. where able to resolve atomic steps with a cantilever and Si-tip attached to the tuning fork [10]. The application of the tuning forks for scanning probe microscopy at low temperatures was demonstrated by Rychen et al. [11, 12, 13]. Recently Giessibl et al. demonstrated atomic resolution on the Si(111)-(7×7) surface using a tuning fork with one prong fixed (qPlus Sensor) [14].

Compared to micromachined Si cantilevers the tuning forks are very stiff. The problems concerning the nonlinearity of the oscillator motion in the interaction potential are reduced due to the high spring constant compared to the interaction forces. The stiffness avoids the snap into contact and thus allows to operate it with lower amplitudes then a cantilever. This simplifies the interpretation of the signals when the short range interactions are investigated. The high stiffness is also of advantage for nano manipulation applications as for example nano-lithography and manipulation. However, it is a disadvantage for the detection of very small forces, and is a danger for the tip to be crashed since the force is not limited by a soft spring.

Since only two electrical contacts are necessary for the operation, piezoelectric tuning forks are simple to integrate in a scanning probe microscope even in a cryogenic environment [13]. They are insensitive to high magnetic fields and operate well at low temperatures. The fact that no light is needed for the deflection detection is important for the investigation of semiconductor heterostructures which show the persistent photo effect. Any light scattered onto the sample would alter its properties permanently.

Since the tuning forks are relatively large and massive, the quality factor is quite robust. In contrast to cantilevers, tuning forks have high quality factors even in ambient conditions ($Q \approx 10'000$) and dynamic force microscopy even in liquids is possible. The perspective to use them as a carrier for sensors like FETs, SETs, SQUIDs and hall sensors makes them attractive especially for the investigation of super- and semiconducting nanostructures in combination with transport experiments.

The direct electromechanical coupling also allows to measure the dissipation power very easily and accurately without the troubles of calibration ($U \times I \times \cos(\theta)$). This is a very powerful advantage of piezoelectric oscillators in dynamic force microscopy.

2 Theory of tuning forks

In this section the models used to deal with the tuning forks are introduced. First an electrical model, the Butterworth-Van Dyke circuit is presented and following the electromechanical coupling via the piezo effect is studied. The influence of asymmetries is then examined with a mechanical model and finally the fundamental limits concerning the dynamic force detection are calculated for the type of tuning fork used in this work.

2.1 Electrical model

Piezoelectric oscillators can be modeled by an electronic equivalent circuit called the Butterworth-Van Dyke circuit (fig. 2 and 3) [15, 16]. The LRC resonator models the mechanical resonance: the inductance stands for the size of the kinetic energy storage, i.e., the effective mass, the capacitance reflects the potential energy storage,i.e., the spring constant and the resistor models the dissipative processes [13]. The parallel capacitance is given by the contacts and cables. The transfer function $Y(\omega) = I(\omega)/U(\omega)$, the so called

admittance is

$$Y(\omega) = \frac{1}{R + \frac{1}{i\omega C} + i\omega L} + i\omega C_0 \quad , \tag{1}$$

and is experimentally measurable. In Figure 3 a Nyquist plot for the transfer function (1) is shown. As for any resonance the curve is a circle but due to the parallel capacitance C_0 its center is shifted along the imaginary axes by $i\omega C_0$. This leads to the typical minimum in the admittance shortly after the maximum in a Bode plot as shown in figure 4. On the resonance the current through the LRC branch flows in phase with the voltage. The current through the parallel capacitance has a phase shift of 90 degree and causes a small phase shift of the total current. However, the admittance of the capacitance C_0 is small compared to the admittance of the LRC branch and can be neglected. If it turns out to be a problem it can be compensated electronically with a bridge circuit.

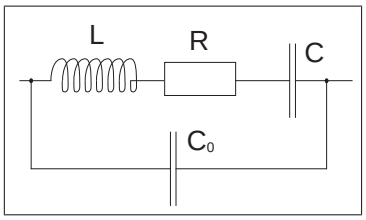

Figure 2: Butterworth-Van Dyke equivalent circuit for a piezoelectric resonator.

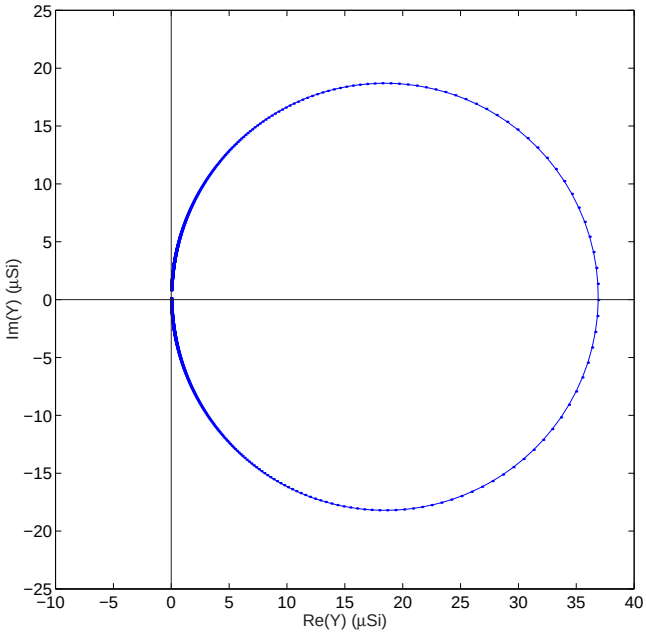

Figure 3: Nyquist plot for a Butterworth-Van Dyke equivalent circuit with parameters as in figure 4: (f_0 = 32765Hz, Q = 62000, C_0 = 1.2pF, L = 8.1kH, R = 27.1kΩ, C = 2.9fF). The frequency is increasing in clockwise direction and the spacing of the data points is 0.01 Hz.

2.2 Electromechanical Coupling

A fit of equation (1) to the experimental data works extremely well. Out of the electrical data the parameters L, R, C and C_0 are obtained. This parameters are not sufficient to determine the mechanical oscillation amplitude. An additional parameter is needed: the piezo-electro-mechanical coupling constant α. It describes the charge separation Q on the electrodes on the piezo material per mechanical deflection x: $[\alpha] = \mathrm{C/m}$. With a simultaneous measurement of the electrical response and the mechanical amplitude with an optical interferometer this constant can be determined [13]. This constant is characteristic for one type of resonator and a modification, for example the attachment of a probe or the change of the environment will not alter this constant. The mechanical amplitude can

always be determined by the current I through the resonator:

$$\begin{aligned} Q &= \alpha x \\ I &= \alpha \dot{x} \\ I_{\mathrm{rms}} &= \alpha \omega x_{\mathrm{rms}} \end{aligned} \tag{2}$$

To model the mechanical resonance, an energetically equivalent mechanical model consisting of one mass and one spring is applied (inset fig. 4a). With the knowledge of the electro mechanical coupling constant α, the mechanical parameters can be determined from the electrical parameters by equating the potential energy $Q^2/2C = kx^2/2$ and the the kinetic energy $LI^2/2 = mv^2/2$:

$$\begin{aligned} L &= m/\alpha^2 \\ 1/C &= k/\alpha^2 \\ R &= \gamma/\alpha^2 \end{aligned} \tag{3}$$

From the electrical and mechanical correspondence the voltage can be identified as the driving force: $F = \alpha U$. Figure 5 shows the electric field in the crystal produced by the electrodes and how they are connected. This configuration detects and excites only movements of the prongs against each other. An interesting point to note is that there is a coupling of the two prongs via the piezoelectric effect. When one prong is deflected it produces a charge separation that in turn produces a voltage and thus deflects the other prong in the opposite direction. Assuming the tuning fork is not connected to any other electronics the charge is converted into a voltage over the capacitance C_0 of the electrodes and the coupling constant is then $\alpha^2/C_0 = 57$ N/m. However, if the tuning fork is connected to cables, the capacitance is much larger and the coupling can be neglected. In the case of a fixed voltage (low impedance) the coupling is zero.

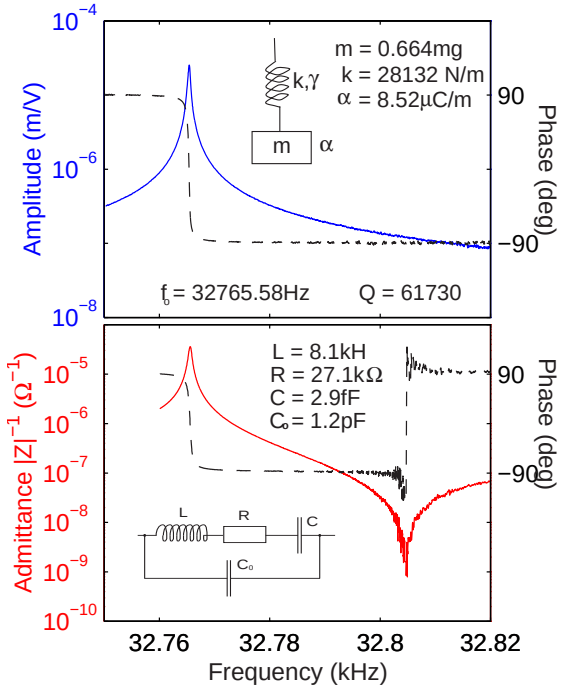

Figure 4: (a) Experimental measurement of the mechanical displacement of the front of a tuning fork prong at room temperature and a pressure of $10^{-}6$ mbar. The inset shows an energetically equivalent mechanical model (both prongs included). (b) The simultaneous experimental measurement of the electrical response. The inset shows the parameters for the electrical equivalent circuit.

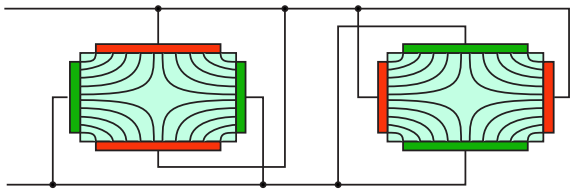

Figure 5: Illustration of the electrical field lines in the cross section of the quartz tuning fork. The electric field along the horizontal direction causes a contraction or dilatation of the quartz in the direction perpendicular to the drawing plane. Only the movement of the two prongs in the mirrored fashion is electrically excitable or detectable.

2.3 Mechanical Model

In the last section a mechanical model was introduced that energetically modeled the proper tuning fork mode and that is appropriate for the determination of the oscillation amplitude. However, questions concerning asymmetries of the tuning fork as they occur when preparing the tuning fork for the dynamic force detection, cannot be answered with this model. A model that takes the two prongs into account has to be applied and is shown in figure 6a. This system has two modes, a symmetric and an antisymmetric one, that are degenerate for vanishing coupling. The coupling splits the two frequencies and the two modes get mixed when the symmetry is broken. This model, however, cannot explain why the counter oscillating mode has a much higher quality factor then the synchronous mode. It is not the appropriate model for a tuning fork since it cannot explain its speciality. The model (b) in figure 6 has a third mass that models the movement of the base. In this model the counter oscillating mode still has a high quality factor because the center of mass stays at rest and all the forces are compensated inside the fork. The synchronous mode however, produces reaction forces in the support of the base and undergoes a much stronger damping. This model also explains the reduction of the quality factor when the symmetry is broken for example by the attachment of a tip to one of the prongs. In the following this model is examined with the help of the Laplace transform and the influence

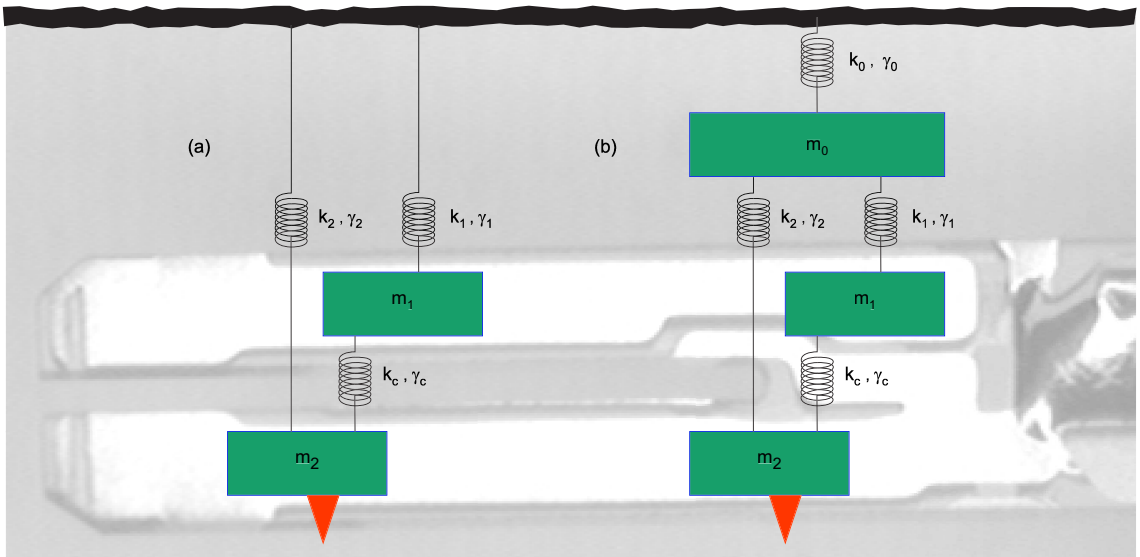

Figure 6: (a) Two coupled oscillators as a mechanical model for the tuning fork. (b) A model with a third mass to explain the influence of asymmetry on the quality factor.

of asymmetry is studied. The equations of motion are

$$\begin{aligned} m_1\, x_1''(t) &= \alpha\, U(t) - k_1\, [x_1(t) - x_0(t)] - k_c\, [x_1(t) - x_2(t)] - \\ &\quad \gamma_1\, \left[x_1'(t) - x_0'(t)\right] - \gamma_c\, \left[x_1'(t) - x_2'(t)\right] \\ m_2\, x_2''(t) &= -\alpha\, U(t) - k_2\, [x_2(t) - x_0(t)] - k_c\, [x_2(t) - x_1(t)] - \\ &\quad \gamma_2\, \left[x_2'(t) - x_0'(t)\right] - \gamma_c\, \left[x_2'(t) - x_1'(t)\right] \\ m_0\, x_0''(t) &= -k_0\, x_0(t) - k_1\, [x_0(t) - x_1(t)] - k_2\, [x_0(t) - x_2(t)] - \\ &\quad \gamma_0\, x_0'(t) - \gamma_1\, \left[x_0'(t) - x_1'(t)\right] - \gamma_2\, \left[x_0'(t) - x_2'(t)\right], \end{aligned} \tag{4}$$

where α is the piezo electric coupling constant and $u(t)$ is the applied voltage and the m's k's and γ's are the masses, spring constants and damping constants respectively. Applying the Laplace transform, the system of differential equations (4) is transformed in a system of algebraic equations which can be solved analytically. The transfer function $T_n(i\omega)$ for the motion of the mass m_n is given by

$$T_n(i\omega) = X_n(i\omega)/U(i\omega)\ , \quad l = 0, 1, 2 \tag{5}$$

where the capitals denote the Laplace transformed variables. The transfer function for the electrical response is given by the relative motion of the two arms:

$$Y(i\omega) = \frac{i\omega C_0 + \alpha i\omega (X_1(i\omega) - X_2(i\omega))}{U(i\omega)} \tag{6}$$

Electrically only the relative motion of the two masses m_1 and m_2 are detected and excited, so that for a symmetric tuning fork only the proper mode is detectable.

This model has too many parameters as to be determined from experimental data. However, the important values (m_i, k_i, γ_i, $i = 1, 2$) are known from the model discussed in sec. 2.1 and the other parameters will just be guessed in order to get a qualitative understanding. For the mass m_0 one has to decide which part of the base will come into motion when reaction forces act on it. This can be just the part of quartz that connects the two prongs, it can be the metallic ring that supports the tuning fork (fig. 1) or it can be all the sensor that is mounted on the piezo tube which itself can show resonances at the frequencies to be considered. When the tuning fork starts to oscillate in a asymmetric manner several different parts of the base and support will come into motion that are connected in a complicated manner. Here m_0 just models the effective mass of all the oscillations that get excited. This effective mass will depend on the frequency and will also be altered at low temperature, but for the purpose of demonstration a fixed value of 5 mg (compared to the mass of 0.33 mg of one prong) is chosen. The spring constant γ_0 is chosen to be 500 kN/m resulting in resonance frequency of around 50 kHz for the mass m_0. The damping constant is now adjusted to have a quality factor of the order of ten for the oscillation of mass m_0: $\gamma_0 = 100$ mNs/m. Finally the following values are used for an example:

$$\left.\begin{aligned} m_1 = m_2 &= 0.33\text{mg} \\ k_1 = k_2 &= 13.79\text{kN/m} \\ \gamma_1 = \gamma_2 &= 1\mu\text{Ns/m} \\ C_0 &= 1.2\text{pF} \\ \alpha &= 4.2\mu\text{C/m} \end{aligned}\right\} \quad \text{measured} \tag{7}$$

$$\left.\begin{aligned} k_c &= 100\text{N/m} \\ \gamma_c &= 0.1\mu\text{Ns/m} \\ m_0 &= 5.0\text{mg} \\ k_0 &= 500\text{kN/m} \\ \gamma_0 &= 100\text{mNs/m} \end{aligned}\right\} \quad \text{estimated} \tag{8}$$

Δm [μg]	f [Hz]	Q	abs(T_d) [m/V]	arc(T_d) [deg]	abs(T_s) [m/V]	arc(T_s) [deg]	abs(T_0) [m/V]	arc(T_0) [deg]
	52503.8	17	$1.92\,10^{-10}$	-180.0	$7.87\,10^{-14}$	54.3	$3.94\,10^{-14}$	-88.9
0.1	31171.6	201	$3.16\,10^{-9}$	-0.0	$8.43\,10^{-11}$	-89.3	$7.52\,10^{-12}$	-93.0
	32767.2	56585	$1.70\,10^{-5}$	-90.0	$2.34\,10^{-8}$	93.6	$2.24\,10^{-9}$	89.5
	52502.1	17	$1.91\,10^{-10}$	-180.0	$7.83\,10^{-13}$	54.3	$3.92\,10^{-13}$	-88.9
1.0	31151.1	202	$3.16\,10^{-9}$	-0.3	$8.44\,10^{-10}$	-89.3	$7.53\,10^{-11}$	-93.0
	32745.2	52855	$1.59\,10^{-5}$	-90.0	$2.19\,10^{-7}$	93.6	$2.09\,10^{-8}$	89.5
	52494.7	17	$1.89\,10^{-10}$	-180.0	$3.83\,10^{-12}$	54.2	$1.92\,10^{-12}$	-88.9
5.0	31054.1	205	$3.17\,10^{-9}$	-6.0	$4.23\,10^{-9}$	-89.4	$3.76\,10^{-10}$	-93.0
	32655.4	20647	$6.17\,10^{-6}$	-90.0	$4.22\,10^{-7}$	93.5	$4.01\,10^{-8}$	89.4
	52485.7	17	$1.87\,10^{-10}$	-180.0	$7.47\,10^{-12}$	54.1	$3.76\,10^{-12}$	-88.9
10.0	30920.6	211	$3.38\,10^{-9}$	-22.3	$8.42\,10^{-9}$	-89.4	$7.44\,10^{-10}$	-93.0
	32559.9	7500	$2.21\,10^{-6}$	-90.1	$2.96\,10^{-7}$	93.3	$2.80\,10^{-8}$	89.3
	52426.5	17	$1.73\,10^{-10}$	-179.7	$3.10\,10^{-11}$	53.3	$1.59\,10^{-11}$	-88.9
50.0	29603.7	299	$1.93\,10^{-8}$	-82.8	$3.48\,10^{-8}$	-89.9	$2.93\,10^{-9}$	-93.1
	32204.8	839	$1.98\,10^{-7}$	-90.7	$9.67\,10^{-8}$	91.8	$9.01\,10^{-9}$	87.9

Table 1: The eigenmodes of the tuning fork model for increasing additional mass on one prong.

A satisfactory agreement with the experimental data in figure 4 is achieved with the parameters (7) and (8) for the calculation of the transfer function (6) shown in figure 7. The poles of the transfer function can be calculated and the location in the $i\omega$-plane determines the eigen frequencies and the damping of the three eigen modes. The model can now be applied to investigate the behavior of the tuning fork when an additional mass is brought onto one of the prongs. To illustrate the eigenmodes the following transfer

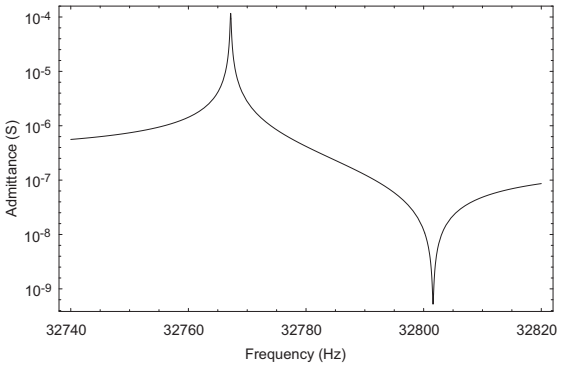

Figure 7: The admittance (6) calculated with the parameters (7) & (8). The curve is in good agreement with the experiment of figure 4.

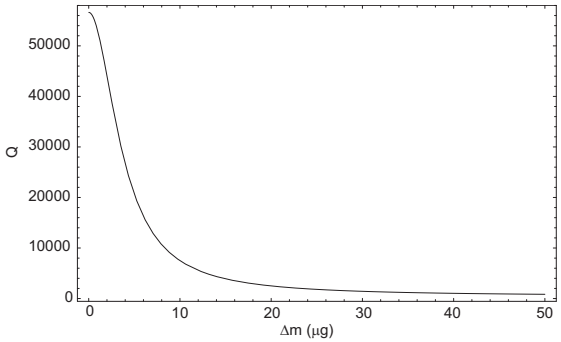

Figure 8: The quality factor is reduced significantly when an additional mass is brought onto one of the prongs (m=0.33mg).

functions will be examined:

$$\begin{aligned} T_d(i\omega) &= \frac{(X_1(i\omega) - X_2(i\omega))}{2U(i\omega)} \\ T_s(i\omega) &= \frac{(X_1(i\omega) + X_2(i\omega) - 2X_0(i\omega)}{2U(i\omega)} \end{aligned} \tag{9}$$

They correspond to the relative motion (T_d) and to the motion of the center of mass of the two prongs relative to mass m_0 (T_s). Table 1 lists the three eigenmodes and the transfer functions (9) for increasing additional mass Δm on prong 1. The remarkable reduction of the quality factor is in good agreement with the practical experience. Figure 8 shows the quality factor as function of the additional mass. The reduction of the frequency of the proper tuning fork mode is also observed experimentally. In conclusion it can be noted that the symmetry of the tuning fork is very important for a high quality factor. Any asymmetry lets reaction forces act on the base of the tuning fork which will cause an additional damping. Furthermore it was shown that the other modes of the tuning fork do generally not interfere with the proper mode or have a much lower quality factor. This is in contrast to the model of two coupled oscillators, where the degeneracy is only slightly resolved by the coupling and the quality factors of both modes are approximatly the same.

2.4 Fundamental Limits

Applying the formalism introduced by Albrecht [17], the fundamental limits for the dynamic force detection with a quartz tuning fork [18] are discussed. As a mechanical model the simple spring mass model shown in figure 4a will be applied. While absolutely correct for the modeling of the proper tuning fork mode, the complications arising from having two prongs are avoided. For the parameters given in figure 4, the thermal white noise drive is $192\,\mathrm{fN}/\sqrt{\mathrm{Hz}}$ at 300 K and $11\,\mathrm{fN}/\sqrt{\mathrm{Hz}}$ at 1 K. Multiplied with the transfer function for the mechanical model, the spectral thermal motion results and is shown in figure 9. Assuming that the deflection detection can detect such small motions, the minimum detectable force gradient [17]

$$F'_{\mathrm{min}} = \sqrt{\frac{4k k_{\mathrm{B}} T B}{\omega_0 Q \langle z_{\mathrm{osc}}^2 \rangle}} \quad . \tag{10}$$

is 4.3 mN/m at 300 K for a detection bandwidth of 100 Hz and a amplitude of 1 nm. The value gets smaller for low temperature (1 K), smaller bandwidth (10 Hz) and larger amplitude (30 nm): $3\,\mu$N/m. However, experimentally this will be hard to realize, since the frequency shift that has to be detected is as low as $3\,\mu$Hz (for the second case). This corresponds to a relative frequency shift of 10^{-10}, which demands for a stability of the reference frequency that exceeds the values of standard equipment. To reach the thermodynamic limit with tuning forks, the deflection detection has to be able to detect the thermal noise off the resonance. For a current to voltage converter with a noise of $100\,\mathrm{fA}/\sqrt{\mathrm{Hz}}$ the thermodynamic limit at room temperature could be reached with a detection bandwidth of about 10 Hz. For the low temperature case, this is not possible with such a current to voltage converter. With a sensitive charge detector with a noise of $0.01\,e/\sqrt{\mathrm{Hz}}$, however, the thermal noise of the tuning fork at low temperature is dominant over a bandwidth of about 50 Hz. In conclusion it can be stated that to reach the thermodynamic limit for force detection, the detection bandwidth has to be narrowed or the quality factor has to be reduced to have the thermal noise of the tuning fork dominant over the deflection detection noise. Experimentally one has to worry also about other sources of noise that could exceed the thermal noise of the tuning fork. For example the noise of the excitation

signal has to be smaller then $1.3\,\mathrm{nV}/\sqrt{\mathrm{Hz}}$ which produces a force αU that corresponds to the thermal white noise drive of $11\,\mathrm{fN}/\sqrt{\mathrm{Hz}}$ at low temperature.

3 Experimental Implementation of Tuning Fork Sensors

In this section the experimental implementation of the tuning fork sensors and the detection techniques are presented. First the assembly of the sensors is described followed by a description of the driving circuit with a Phase Locked Loop and a description of the low temperature preamplifier.

3.1 Preparation of Tuning Fork Sensors

Tuning forks are produced industrially and are packed in an evacuated steel casing where they show quality factors of about 30'000.[1] The casing is removed at the base and the quality factor drops to about 10'000 in ambient conditions [19]. A thin metal wire is glued to one of the prongs and then electro-chemically etched to form a sharp tip (fig. 10a). The preparation of metallic tip for scanning probes is well described in the literature [20, 21, 22, 23], and in ref. [24] specially the etching of the thin wires used for the tuning fork tips. For the attachment of the tip it is very important to disturb the symmetry of the tuning fork as little as possible (sec. 2.3). The metal wire has a diameter of only 15μm to minimize the additional weight on one prong. A small drop of glue on the other prong can help to compensate for the additional mass. The wire is either connected with one of the tuning fork electrodes causing an additional mass of about $1.5\,\mu$g, or is is separately contacted causing an additional weight of up to $50\,\mu$g. In the latter case the metal wire loop causes also an additional spring and damping for the one prong. To keep the wire loop as short as possible it is attached to a pillar mounted closely to the end of the tuning fork

[1] All quantitative data are related to the type shown in figure 1

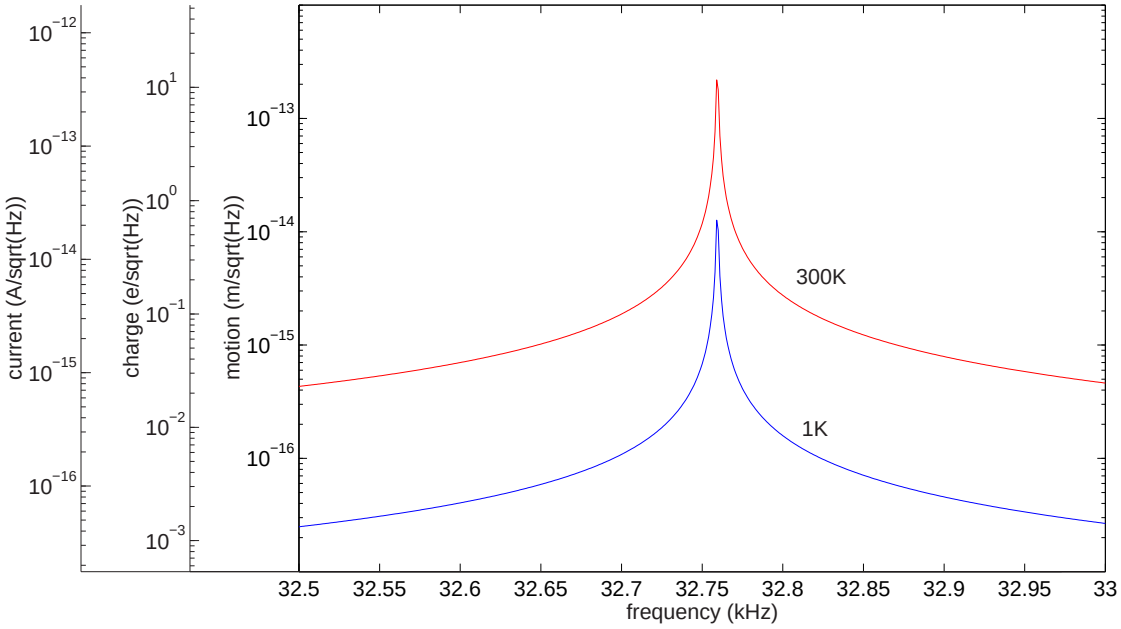

Figure 9: The thermal motion of a tuning fork at room temperature (300K) and at 1K. The motion is converted into a charge via the piezo-electro-mechanical coupling constant α and into a current by multiplying the charge with the frequency.

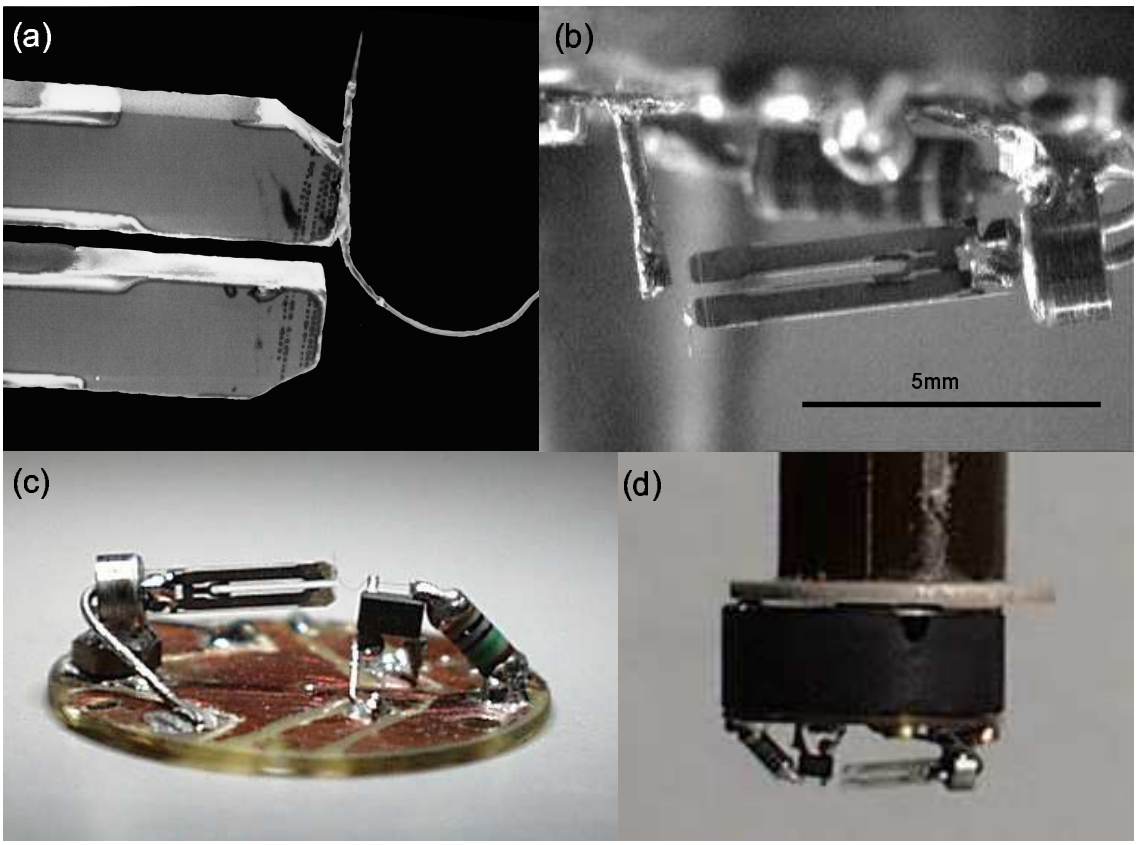

Figure 10: Quartz tuning fork sensors for the dynamic force detection. A thin metal wire is attached to one prong and etched or cut to form a sharp tip (a). The tip is separately contacted to a current to voltage converter (b) or to a field effect transistor acting as a low input capacitance preamplifier (c). The sensor plate is mounted on the puck of the xy-table with six screws which also serve for the electrical contacts (c).

prong (fig. 10b). Tuning fork sensors with separately contacted tip show quality factors of about 50'000 in vacuum at 4.2K

With a separately contacted tip it is comfortable to perform tunneling or capacitance measurements. For the small signals as they occur in capacitance measurements and in Kelvin Probe Microscopy, a Field Effect Transistor (FET) that can be mounted very closely to the tip is advantageous (sec. 3.3). The FET has to be mounted parallel to the magnetic field to minimize its effects on the electron gas of the FET. Within this work, only the configuration where the tip oscillates perpendicular to the sample was tried out, but also the shear force configuration, where the tip oscillates parallel to the sample is well established [7].

3.2 The Phase Locked Loop

The frequency shift of the tuning fork is much smaller than that of traditional cantilevers when the tip interacts with the sample because the spring constant is much higher. This demands for a frequency demodulation [25] with high resolution and stability. Since the tuning fork resonance is at a quite low frequency (33kHz), digital signal processing (DSP) can be applied. This is of great advantage because no analog devices can have a relative accuracy of 10^{-9} or better. As shown in figure 4 the phase between the excitation signal and the current through the fork as a function of the frequency is very steep at the resonance (about 180 degree/Hz). This allows to detect any shifts in the resonance

frequency very sensitively. With a controller the excitation frequency is then automatically adjusted to maintain the phase at the value of the resonance. This is the idea of the PLL and is schematically shown in figure 11. This PLL is put together with standard laboratory equipment and special software for the integration and automation. This has the advantage that all the parameters like the detection bandwidth and PI parameters can easily and transparently be adjusted.

The deviation of the phase is detected with a digital two channel lock-in amplifier (SRS 830) which is synchronized by a digital signal from the frequency generator. The lock-in amplifier generates two orthogonal sinus signals as reference for the two channels. The phase of this reference signals with respect to the external synchronization signal can be shifted by an arbitrary value and is adjusted to have the x-reference signal in phase with the signal of the tuning fork at the resonance. Ideally this phase shift would be zero (fig. 3) but the current-to-voltage converters and the long coax cables cause an additional phase shift. The output of the y-channel which indicates any deviation from the resonance, is fed into a PI-controller to control the frequency to the resonance.

The frequency generator (Yokogawa FG300) employs the Direct Data Synthesis (DDS) and has a phase register of 48bit and a clock rate of 40MHz. The span of the frequency modulation range is typically configured to be 100mHz/V and the resolution for the frequency shift is then about 100μHz. For very sensitive force detection the parameters can be adjusted to achieve resolutions of the order of 1μHz. However, the stability of the reference frequency is specified to be 100μHz/^{o}C and for the ultimate frequency shift detection an external reference frequency with a temperature controlled quartz oscillator (OCXO) or an atomic clock should be employed.

As an additional feature the oscillation amplitude of the tuning fork is detected with the x-channel of the lock-in amplifier and the output signal is kept constant by a second feedback loop which controls the amplitude of the excitation signal. This simplifies the interpretation of the different recorded signals, since the mechanical oscillation amplitude of the tuning fork can be assumed to be constant. Second, the transients are avoided that occur in response to a sudden change in the damping and could last up to seconds for high quality factors.

The PLL provides two signals that indicate the frequency shift and the excitation amplitude. Both signals can be used to control the probe sample distance by the z-feedback controller.

The power dissipated in the tuning fork is the product of the current and the voltage multiplied by the cosine of the phase angle between the two signals. The phase angle is zero

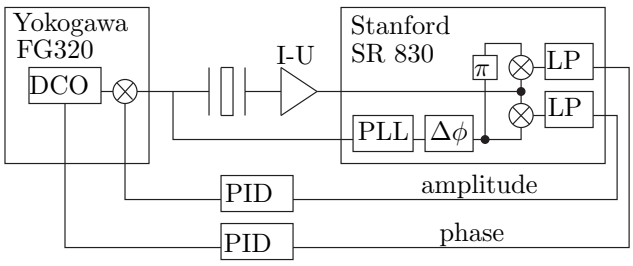

Figure 11: A phase locked loop is employed to measure the frequency shift of the tuning fork. The driving signal is generated by an digital function generator employing the direct data synthesis method (DDS). The motion of the tuning fork is detected with a current to voltage amplifier and analyzed with a digital two channel Lock-in amplifier. Its output signals indicate the mechanical amplitude and the phase shift, which is used to control the frequency to the resonance. The mechanical amplitude is kept fix by controlling the amplitude of the excitation signal of the function generator.

on the resonance and is locked by the PLL. The current is kept constant by the amplitude controller and therefore the amplitude of the excitation signal is a direct measure for the power dissipation. Any additional damping caused by probe sample interactions can be detected very sensitively in this manner. Additional power dissipations of the order of 1fW have been detected. This corresponds to an energy loss of 0.2eV per cycle of the tuning fork with a typical oscillation energy of the order of 10^5eV (for 1nm amplitude).

3.3 The Low Temperature Preamplifier

In both, scanning capacitance and in Kelvin probe microscopy, very small amounts of charges are induced on the tip. This charge elevates the potential of the tip depending on the capacitance to the rest of the world. When the tip is connected via a coax cable to a current-to-voltage converter then the cable capacitance is of the order of 100 - 400pF depending of the length of the cable. The current-to-voltage converter detects the small rise in voltage and compensates it by letting the current flow over the feedback resistor. Only a small fraction of about 1% of the charge that is induced on the tip is brought onto the gate of the first input transistor of the operational amplifier which has typical input capacitances of the order of 1pF. The rest of the charge is used to fill the cable capacitance. To overcome this problem it is desirable to have the preamplifier as close to the experiment as possible eliminating the need of propagating very small signals over long coax cables. The low temperatures, the high magnetic fields, the limited space and the low cooling power are not forming the ideal environment for a preamplifier. However, GaAs-Field-Effect-Transistors (FETs) work even at low temperatures and when mounted parallel to the magnetic field, it is possible to operate them even at 10 Tesla. The power consumption can be reduced to reasonably low values but at the expense of the signal to noise ratio.

In figure 10c a tuning fork sensor with a GaAs FET connected to the tip is shown. For the detection of the tuning fork itself also a cryo-preamplifier can be used if very low oscillation amplitudes are desired.

Figure 12 shows the circuit used to drive the preamplifier. The conductivity of the channel is measured with a current-to-voltage converter keeping the source-drain voltage U_{SD} fixed. Compared to the established source follower circuit, this has the advantage that the FET can also be operated in the ohmic regime and thus allowing an operation

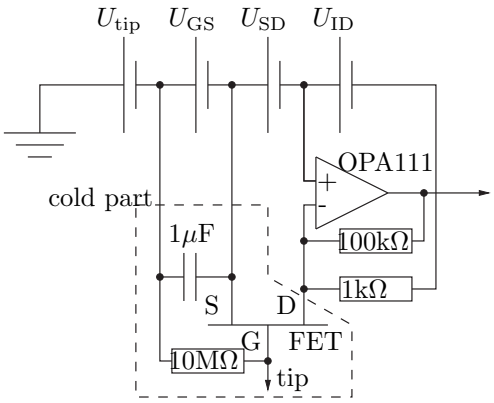

Figure 12: The low temperature preamplifier allows to detect small signals very close to the experiment providing a small input capacitance. The conductance of the channel is measured with a current-to-voltage converter keeping the Source-Drain voltage fixed and thus allowing an operation at much lower dissipation power.

with smaller dissipation power. The circuit is powered by batteries and its potential U_{tip} relative to common ground can be externally defined within ±100V. The output signal is optically coupled out allowing a completely isolated detection circuit. The whole circuit and with it the tip can also be modulated with frequencies up to 100kHz without affecting the output signal except for the capacitive coupling of the tip to its surrounding.

The working point of the FET can be adjusted by the Gate-Source voltage U_{GS} and the Source-Drain voltage U_{SD}. To account for the changing properties of the FET with varying temperature and magnetic field, the characteristics can be measured in situ allowing the optimum operation point to be found by giving an additional condition like the maximum power dissipation or the minimum signal to noise ratio.

The dc-current through the channel of the FET flows over the 1kΩ resistor, and the small ac-current in addition to the dc-current is taken by the current-to-voltage converter. The voltage U_{ID} has to be adjusted so that no dc-current will cause the current to voltage converter to come into overload.

The application of the FET as a preamplifier close to the tip allows to detect very small signals. This is especially advantageous for the Kelvin probe experiments where any small signal has to be nulled by a bias voltage between the tip and sample. The calibration and the stability of the amplifier is not important for this application. However, for the scanning capacitance microscopy the small variations of the tip-sample capacitance have to be detected in a large background signal from stray capacitances. In this case the gain of the amplifier has to be stabilized with an accuracy better than $10^{-4} - 10^{-6}$.

References

[1] J. Rychen. *Combined Low-Temperature Scanning Probe Microscopy and Magneto-Transport Experiments for the Local Investigation of Mesoscopic Systems.* PhD thesis, Swiss Federal Institute of Technology ETH, 2001.

[2] P. Günther, U. Ch. Fischer, and K. Dransfeld. Scanning near-field acoustic microscopy. *Applied Physics B*, 48:89–92, 1989.

[3] K. Karrai and Robert Grober. Piezoelectric tip-sample distance control for near field optical microscopes. *Appl. Phys. Lett.*, 66(14):1842–1844, April 1995.

[4] A. G. Ruiter, J. A. Veerman, K. O. van der Werf, and N. F. van Hulst. Dynamic behavior of tuning fork shear-force feedback. *Appl. Phys. Lett.*, 71(1):28–30, July 1997.

[5] A. G. T. Ruiter, J. A. Veerman K. O. van der Werf, M. F. Garcia-Parajo, W. H. J. Rensen, and N. F. van Hulst. Tuning fork shear-force feedback. *Ultramicroscopy*, 71:149–157, 1998.

[6] W. A. Atia and C. C. Davis. A phase-locked shear-force microscope for distance regulation in near-field optical microscopy. *Appl. Phys. Lett.*, 70(4):405–407, January 1997.

[7] K. Karrai and I. Tiemann. Interfacial shear force microscopy. *Phys. Rev. B*, 62(19):13174–13181, November 2000.

[8] H. Edwards, L. Taylor, W. Ducncan, and A. J. Melmed. Fast, high-resolution atomic force microscopy using a quartz tuning fork as actuator and sensor. *J. Appl. Phys.*, 82(3):980–984, August 1997.

[9] M. Todorovic and S. Schultz. Magnetic force microscopy using nonoptical piezoelectric quartz tuning fork detection design with applications to magnetic recording studies. *J. Appl. Phys.*, 83(11):6229–6231, June 1998.

[10] W. H. J. Rensen adn N. F. van Hulst. Atomic steps with tuning fork based noncontact atomic force microscopy. *Appl. Phys. Lett.*, 75(11):1640–1642, September 1999.

[11] J. Rychen, T. Ihn, P. Studerus, A. Herrmann, K. Ensslin, H. J. Hug, P. J. A. van Schendel, and H. J. Güntherodt. Force-distance studies with piezoelectric tuning forks below 4.2k. *Appl. Surf. Sci.*, 157(4):290–294, April 2000.

[12] J. Rychen, T. Ihn, P. Studerus, A. Herrmann, and K. Ensslin. A low-temperature dynamic mode scanning force microscope operating in high magnetic fields. *Rev. Sci. Instr.*, 70(6):2765–2768, June 1999.

[13] J. Rychen, T. Ihn, P. Studerus, A. Herrmann, K. Ensslin, H. J. Hug, P. J. A. van Schendel, and H. J. Güntherodt. Operation characteristics of piezoelectric quartz tuning forks in high magnetic fileds at liquid helium temperatures. *Rev. Sci. Instr.*, 71(3), March 2000.

[14] F. J. Giessibl. High-speed force sensor for force microscopy and profilometry utilizing a quartz tuning fork. *Appl. Phys. Lett.*, 73(26):3956–3958, December 1998.

[15] A. Arnau, T. Sogorb, and Y. Jiménez. A continous motional series resonant frequency monitoring circuit and a new method of determining butterworth-van dyke parameters of a quartz crystal microbalance in fluid media. *Rev. Sci. Instr.*, 71(6):2563–2571, June 2000.

[16] Yoshiro Tomikawa, H. Miura, and S. B. Dong. Analysis of electrical equivalent circuit elements of piezo tuning forks by the finite element method. *IEEE transactions on sonics and ultrasonics*, SU-25(4):206–212, July 1978.

[17] T. R. Albrecht, P. Grütter, D. Horne, and D. Rugar. Frequency modulation detection using high-q cantilevers for enhanced force microscope sensitivity. *J. Appl. Phys.*, 69(2):668–673, January 1991.

[18] Robert D. Grober, Jason Acimovic, Jim Schuck, Dan Hessman, Peter J. Kindelmann, Joao Mespanha, A. Stephen Morse, Khaled Karrai, Ingo Tiemann, and Stephan Manus. Fundamental limits to force detection using quartz tuning forks. *Rev. Sci. Instr.*, 71(7):2776–2780, July 2000.

[19] Christian Steiner. Resonanzverhalten von Quartz-Stimmgabeln. Diplomarbeit, Institut für Fetskörperphysik, ETH Zürich, Prof. Dr. K. Ensslin, 1998.

[20] A. H. Sorensen, U. Hvid, M. W. Mortensen, and K. A. Morch. Preparation of platin/iridium scanning probe microscopy tips. *Rev. Sci. Instr.*, 70(7):3059–3067, July 1999.

[21] I. H. Musselman and P. E. Russell. Platin/iridium tips with controlled geometry for scanning tunneling microscopy. *J. Vac. Sci. Technol. A*, 8(4):3558–3562, July 1990.

[22] L. A. Nagahara, T. Thundat, and S. M. Lindsay. Preparation and characterization of STM tips for electrochemical studies. *Rev. Sci. Instr.*, 60(10):3128–3130, October 1989.

[23] J. P. Ibe, P. P. Bey, S. S. Barndow, R. A. Brizzolara, N. A. Burnham, D. P. DiLella, K. P. Lee, C. R. K. Marrian, and R. J. Colton. On the electrochemical etching of tips for scanning tunneling microscopy. *J. Vac. Sci. Technol. A*, 8(4):3570–3575, July 1990.

[24] Peter Vorburger. Construction of a scanning force microscope and force-distance measuremements on gold and graphite surfaces. Diplomarbeit, Institut für Fetskörperphysik, ETH Zürich, Prof. Dr. K. Ensslin, 1999.

[25] U. Dürig, H. R. Steinauer, and N. Blanc. Dynamic force microscopy by means of the phase-controlled oscillator method. *J. Appl. Phys.*, 82(8):3641–3651, October 1997.